ACADEMIC PRESS

Available online at www.sciencedirect.com

SCIENCE DIRECT®

Journal of Sound and Vibration 260 (2003) 19–44

JOURNAL OF SOUND AND VIBRATION

www.elsevier.com/locate/jsvi

Free vibration analysis of planar curved beams by wave propagation

B. Kang[a,*], C.H. Riedel[b], C.A. Tan[c]

[a] *Mechanical Engineering Department, Indiana University-Purdue University, Fort Wayne, IN 46805-1499, USA*
[b] *Mechanical Engineering Department, Lawrence Technological University, Southfield, MI 48075-1058, USA*
[c] *Mechanical Engineering Department, Wayne State University, Detroit, MI 48202, USA*

Received 14 September 2001; accepted 8 April 2002

Abstract

In this paper, a systematic approach for the free vibration analysis of a planar circular curved beam system is presented. The system considered includes multiple point discontinuities such as elastic supports, attached masses, and curvature changes. Neglecting transverse shear and rotary inertia, harmonic wave solutions are found for both extensional and inextensional curved beam models. Dispersion equations are obtained and cut-off frequencies are determined. Wave reflection and transmission matrices are formulated, accounting for general support conditions. These matrices are combined, with the aid of field transfer matrices, to provide a concise and efficient method for the free vibration problem of multi-span planar circular curved beams with general boundary conditions and supports. The solutions are exact since the effects of attenuating wave components are included in the formulation. Several examples are presented and compared with other methods.

1. Introduction

The vibration of planar curved beams, arches and rings have been the subject of numerous studies due to their wide variety of potential applications, such as bridges, aircraft structures, and turbomachinery blades. These structures are modelled as either extensional (including the extension of the neutral axis) or inextensional (neglecting the extension of the neutral axis), with Euler–Bernoulli and Timoshenko curved beams having been formulated for each model. Literature reviews on the vibration of curved beams, rings and arches are found in Refs. [1–3].

*Corresponding author. Tel.: +1-219-481-5712; fax: +1-219-481-5728.
E-mail addresses: kang@engr.ipfw.edu (B. Kang), riedel@ltu.edu (C.H. Riedel), tan@tan.eng.wayne.edu (C.A. Tan).

0022-460X/03/$ - see front matter
PII: S0022-460X(02)00898-2

Many methods have been employed to study the free vibration of curved members. Den Hartog [4] obtained the natural frequencies of circular arcs with fixed and hinged boundary conditions using the Rayleigh–Ritz method. Ball [5] utilized the finite difference method for the dynamic analysis of rings. Many studies, such as Rao and Sundararajan [6] and Tufekci and Arpaci [7], solve the equations of motion governing the in-plane vibration for classical boundary conditions. Wang and Lee [8] presented a dynamic slope-deflection method for the free vibration of multi-span circular frames. Using a transfer matrix approach, Bickford and Strom [9] obtained the natural frequencies and mode shapes for both the in-plane and out-of-plane vibrations of plane curved beams accounting for shear deformation, rotary inertia and extension of the neutral axis. Issa et al. [10] formulated a general dynamic stiffness matrix for a circular curved member including the effects of transverse shear, rotary inertia and the extensional effect of the neutral axis. Chidamparam and Leissa [11] incorporated the Galerkin method to study the in-plane free vibrations of extensional and inextensional loaded circular arches. Mau and Williams [12] solved the arch vibration problem using the Green function. Numerous studies have developed curved beam finite elements for both Timoshenko and Euler–Bernoulli curved beam models [13–19].

Another very useful method in vibration analysis is the wave propagation approach. This method makes use of the well-known fact that the vibration of elastic structures such as strings, beams, and plates can be described in terms of waves propagating and attenuating in waveguides [20,21]. The compact and systematic methodology of this approach allows the analysis of complex structures such as multi-span beams, trusses, aircraft panels with periodic supports, as well as revealing important physical characteristics associated with the vibration of the structure [22,23]. One of the earliest investigations of wave motion in curved beams was done by Love [24]. He assumed a constant radius of curvature and neglected the extension of the neutral axis. Wittrick [25] studied the wave propagation in helical springs while Farshad [26] investigated wave propagation in prestressed curved rods. Morley [27] considered elastic waves in a curved rod, accounting for shear deformation, rotary inertia and extension of the neural axis. Phase velocity equations show that there is no significant interaction between extension and flexure for the case of slight curvature. Graff [28] developed equations for a ring, accounting for extensional, shear and rotary inertia. Dispersion curves are presented showing the effects of curvature, shear, and inertia on the wave propagation.

The above-cited curved beam wave analysis studies all focus on wave propagation characteristics. Mallik and Mead [29] appear to be one of the first to utilize wave analysis techniques in determining natural frequencies and modeshapes of curved members. They determined propagation constants and receptance functions to study circular rings on multiple, equi-spaced radial supports. In their study, only full rings and classical support conditions were considered. The purpose of this paper is to use wave analysis techniques, specifically wave reflection and transmission matrices, along with field transfer matrices, to develop a systematic method for analyzing the free vibration of planar (extensional and inextensional) circular curved beams. The approach will not only be systematic, but will also account for multiple spans with discontinuities and general boundary conditions. The principle behind the present approach is called the phase closure principle [30] (also called the wave-train closure principle [21]). This principle states that if the phase difference between incident and reflected waves is an integer multiple of 2π, then the waves propagate at a natural frequency and their motions constitute a vibration mode.

The manuscript is organized as follows. The governing equations of motion of a circular curved beam, neglecting transverse shear and rotary inertia effects, are presented in Section 2 and their general wave solutions over the entire frequency spectrum are formulated in Section 3. In Section 4, the wave reflection and transmission matrices are derived for the planar circular curved beam under various point supports. The supports can include translation and rotational springs as well as an attached mass with rotational inertia. Knowing the reflection and transmission matrices, Section 5 illustrates a systematic approach, utilizing field transfer matrices, to apply these matrices in solving the free vibration of multiple span curved beams with discontinuities and general boundary conditions. Four examples are presented in Section 6 to illustrate the proposed methodology and compare it with other methods. Summary and conclusions are presented in Section 7.

2. Governing equations of motion

Consider a thin curved beam, as shown in Fig. 1, where M is the bending moment, N the tensile force, and V the shear force. Neglecting the effects of rotary inertia, shear deformations, and damping, the coupled equations of motion governing the radial displacement, W, and the tangential displacement, U, of the centroidal axis are

$$\frac{EI}{R^3}\frac{\partial^3}{\partial\theta^3}\left(U-\frac{\partial W}{\partial\theta}\right)-\frac{EA}{R}\left(W+\frac{\partial U}{\partial\theta}\right)=\rho AR\frac{\partial^2 W}{\partial T^2}, \tag{1a}$$

$$\frac{EI}{R^3}\frac{\partial^2}{\partial\theta^2}\left(U-\frac{\partial W}{\partial\theta}\right)+\frac{EA}{R}\frac{\partial}{\partial\theta}\left(W+\frac{\partial U}{\partial\theta}\right)=\rho AR\frac{\partial^2 U}{\partial T^2}, \tag{1b}$$

where E denotes Young's modulus, I the second moment of inertia of the cross-section about the centroid, θ the angular co-ordinate, R the constant radius of curvature for the given range of angle

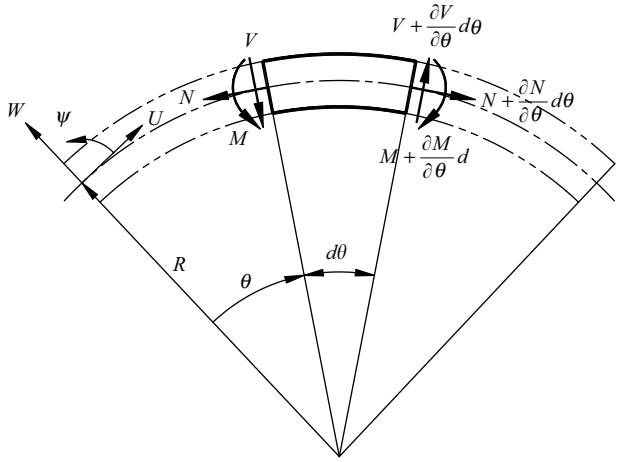

Fig. 1. Schematic of a curved beam and sign conventions.

θ, A the cross-sectional area, ρ the mass density, T the time variable. Details of deriving these equations of motion are found in Refs. [11,20].

Introduce the following non-dimensional variables and parameters:

$$u = \frac{U}{R}, \qquad w = \frac{W}{R}, \qquad t = \frac{T}{T_0}, \qquad T_0 = R^2\sqrt{\frac{\rho A}{EI}}, \qquad k^2 = \frac{I}{AR^2}, \tag{2}$$

where T_0 is a characteristic time constant and k is the curvature parameter [11]. Applying Eq. (2) to Eq. (1) yields the normalized equations of motion:

$$k^2\frac{\partial^3}{\partial\theta^3}\left(u - \frac{\partial w}{\partial\theta}\right) - \left(w + \frac{\partial u}{\partial\theta}\right) = k^2\frac{\partial^2 w}{\partial t^2}, \tag{3a}$$

$$k^2\frac{\partial^2}{\partial\theta^2}\left(u - \frac{\partial w}{\partial\theta}\right) + \frac{\partial}{\partial\theta}\left(w + \frac{\partial u}{\partial\theta}\right) = k^2\frac{\partial^2 w}{\partial t^2}. \tag{3b}$$

3. Harmonic wave solutions

A vibrating beam is a dispersive medium. In a dispersive medium, the phase velocity is not constant. As such, the simple wave solution of the form $f(s \pm ct)$ with constant phase velocity c does not satisfy Eq. (3). Therefore, to assess the wave propagation in the curved beam model, it is first necessary to determine the condition under which the following wave solutions,

$$W(\theta, T) = C_W e^{i(\Gamma R\theta - \Omega T)}, \tag{4a}$$

$$U(\theta, T) = C_U e^{i(\Gamma R\theta - \Omega T)}, \quad i = \sqrt{-1}, \tag{4b}$$

or in a non-dimensional form,

$$w(\theta, T) = C_w e^{i(\gamma\theta - \omega t)}, \tag{5a}$$

$$u(\theta, t) = C_u e^{i(\gamma\theta - \omega t)}, \quad 0 \leqslant \theta \leqslant 2\pi, \tag{5b}$$

satisfy the equations of motion, where γ and ω are the non-dimensionalized wavenumber and frequency, respectively, and defined as

$$\gamma = R\Gamma, \quad \omega = \Omega T_0. \tag{5c}$$

Note that the wave amplitudes C_w and C_u in Eqs. (5) are not independent and their amplitude ratio is

$$\alpha = \frac{C_u}{C_w} = \frac{i\gamma(1 + \gamma^2 k^2)}{\gamma^2(1 + k^2) - k^2\omega^2}. \tag{6}$$

Substituting the harmonic solutions (5) into Eq. (3) gives

$$\begin{bmatrix} 1 + k^2(\gamma^4 - \omega^2) & i\gamma(1 + \gamma^2 k^2) \\ i\gamma(1 + \gamma^2 k^2) & -\gamma^2 + k^2(\omega^2 - \gamma^2) \end{bmatrix} \begin{Bmatrix} C_w \\ C_u \end{Bmatrix} = 0. \tag{7}$$

Since the determinant of the matrix in Eq. (7) must vanish for non-trivial solutions, one can obtain the dispersion equation in terms of the wavenumber γ,

$$\gamma^6 + (-2 - k^2\omega^2)\gamma^4 + \{1 - (1 + k^2)\omega^2\}\gamma^2 + (k^2\omega^2 - 1)\omega^2 = 0. \tag{8}$$

It can be readily seen that if $k = 0$, Eq. (8) becomes identical to the dispersion equation of an inextensional curved beam for which $w = -\mathrm{d}u/\mathrm{d}\theta$. In this case, Eq. (3) reduces to

$$\frac{\partial^3}{\partial\theta^3}\left(u - \frac{\partial w}{\partial\theta}\right) = \frac{\partial^2 w}{\partial t^2}, \tag{9a}$$

$$\frac{\partial^2}{\partial\theta^2}\left(u - \frac{\partial w}{\partial\theta}\right) = \frac{\partial^2 u}{\partial t^2}. \tag{9b}$$

It should be noted that for a given cross-sectional geometry, there is a limiting value of k for which Eq. (8) is valid. This is due to the fact that for large values of k, the vibration modes may not be realistic due to the wavelengths being small in comparison to the thickness of the beam. For example, the limiting value of k is $\frac{1}{2}$ for a circular beam, meaning that R is equal to the radius of the cross-section of the beam.

Shown in Fig. 2 is the general behavior of the positive branches of the frequency spectrum for the extensional ($k = 0.0289$, see Figs. 2(a) and (b)) and inextensional ($k = 0$, see Figs. 2(c) and (d)) curved beam models. Comparing Figs. 2(a) and (c), it is clearly seen that there exists an additional frequency spectrum emerging from a non-zero frequency for the extensional curved beam model. This additional frequency spectrum represents the coupled flexural and extensional mode, with the extensional mode dominating. The non-zero *cut-off frequency*, denoted by ω_c, defining this additional frequency spectrum can be readily identified by taking the long-wavelength limit of Eq. (8); i.e.,

$$\lim_{\gamma\to 0}(8) = (k^2\omega^2 - 1)\omega^2 = 0, \tag{10}$$

which gives two roots: $\omega_c = 0$ and $1/k$. Considering the first root, as ω approaches $\omega_c = 0$, Eq. (6) reveals that $C_w = 0$ and $C_u \neq 0$, and therefore Eq. (4) gives $w = 0$ and $u = C_u$. Thus, there is only tangential motion and no radial displacement. Considering the second root, as ω approaches to $\omega_c = 1/k$, $C_w \neq 0$ and $C_u = 0$, so that $w = C_w \mathrm{e}^{-(\mathrm{i}/k)t}$ (standing wave) and $u = 0$, resulting in only radial motion and no tangential displacement. Thus, $\omega = \omega_c = 1/k$ is the frequency when the wavelength of extensional waves in a straight rod is equal to the circumference, $2\pi R$, and is known as the *ring frequency* in cylindrical shell dynamics [31].

The six roots (essentially three complex conjugates) of Eq. (8) can be obtained in a closed form by transforming Eq. (8) into a cubic equation. This results in four different sets of roots, indicating that four distinct wave motions exist in an extensional curved beam depending on the vibration frequency ω and the curvature parameter k. Hence, it is possible to classify the general wave solutions into four different cases as follows:

Case I (*all six γ's are real*):

$$w(\theta, t) = (C^+_{w1}\mathrm{e}^{-\mathrm{i}\gamma_1\theta} + C^+_{w2}\mathrm{e}^{-\mathrm{i}\gamma_2\theta} + C^+_{w3}\mathrm{e}^{-\mathrm{i}\gamma_3\theta} + C^-_{w1}\mathrm{e}^{\mathrm{i}\gamma_1\theta} + C^-_{w2}\mathrm{e}^{\mathrm{i}\gamma_2\theta} + C^-_{w3}\mathrm{e}^{\mathrm{i}\gamma_3\theta})\mathrm{e}^{-\mathrm{i}\omega t}, \tag{11a}$$

$$u(\theta, t) = (C^+_{u1}\mathrm{e}^{-\mathrm{i}\gamma_1\theta} + C^+_{u2}\mathrm{e}^{-\mathrm{i}\gamma_2\theta} + C^+_{u3}\mathrm{e}^{-\mathrm{i}\gamma_3\theta} + C^-_{u1}\mathrm{e}^{\mathrm{i}\gamma_1\theta} + C^-_{u2}\mathrm{e}^{\mathrm{i}\gamma_2\theta} + C^-_{u3}\mathrm{e}^{\mathrm{i}\gamma_3\theta})\mathrm{e}^{-\mathrm{i}\omega t}. \tag{11b}$$

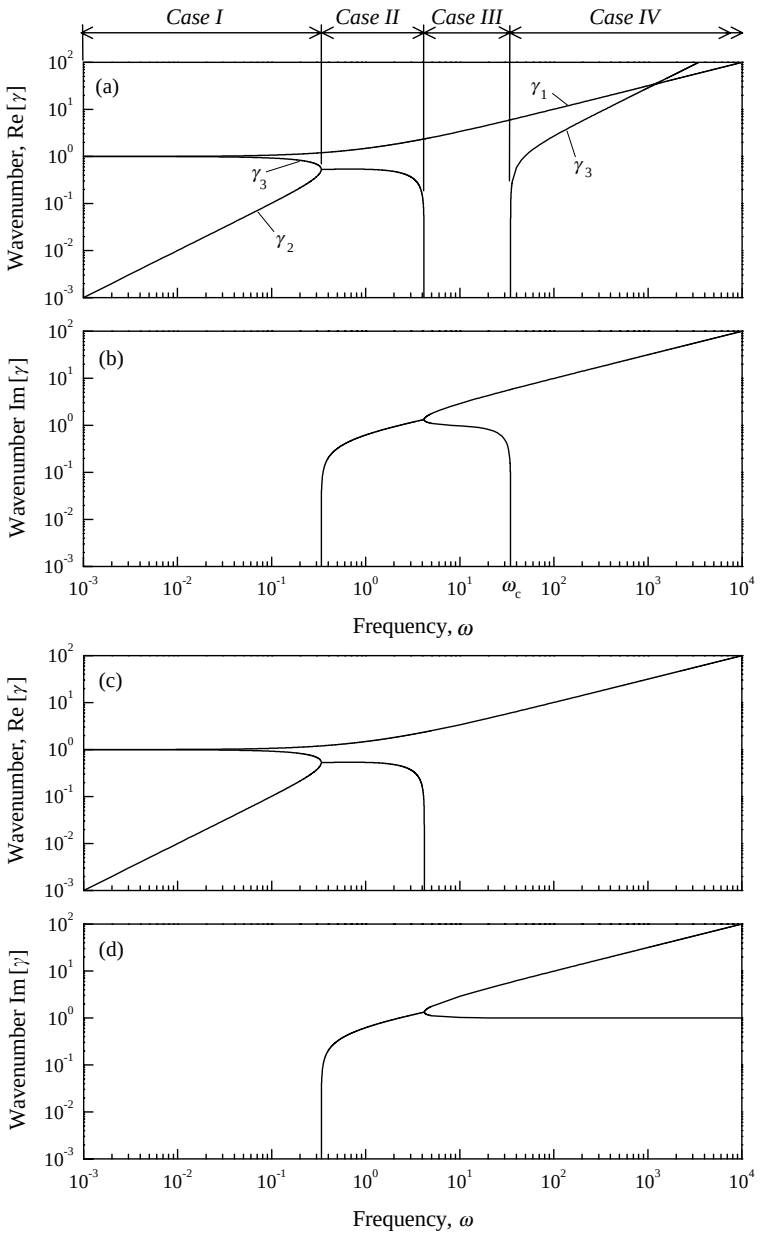

Fig. 2. Frequency spectra of a curved beam for which (a) real and (b) imaginary branches when $k = 0.0289$ (extensional); (c) real and (d) imaginary branches when $k = 0$ (inextensional).

Case II (*two γ's are real and four γ's are complex*):

$$w(\theta, t) = (C_{w1}^{+}e^{-i\gamma_1\theta} + C_{w2}^{+}e^{-i\gamma_2\theta} + C_{w3}^{+}e^{-i\gamma_3\theta} + C_{w1}^{-}e^{i\gamma_1\theta} + C_{w2}^{-}e^{i\gamma_2\theta} + C_{w3}^{-}e^{i\gamma_3\theta})e^{-i\omega t}, \quad (12a)$$

$$u(\theta, t) = (C_{u1}^{+}e^{-i\gamma_1\theta} + C_{u2}^{+}e^{-i\gamma_2\theta} + C_{u3}^{+}e^{-i\gamma_3\theta} + C_{u1}^{-}e^{i\gamma_1\theta} + C_{u2}^{-}e^{i\gamma_2\theta} + C_{u3}^{-}e^{i\gamma_3\theta})e^{-i\omega t}. \quad (12b)$$

Case III (*two γ's are real and four γ's are imaginary*):

$$w(\theta,t) = (C_{w1}^{+}e^{-i\gamma_1\theta} + C_{w2}^{+}e^{i\gamma_2\theta} + C_{w3}^{+}e^{i\gamma_3\theta} + C_{w1}^{-}e^{i\gamma_1\theta} + C_{w2}^{-}e^{-i\gamma_2\theta} + C_{w3}^{-}e^{-i\gamma_3\theta})e^{-i\omega t}, \quad (13a)$$

$$u(\theta,t) = (C_{u1}^{+}e^{-i\gamma_1\theta} + C_{u2}^{+}e^{i\gamma_2\theta} + C_{u3}^{+}e^{i\gamma_3\theta} + C_{u1}^{-}e^{i\gamma_1\theta} + C_{u2}^{-}e^{-i\gamma_2\theta} + C_{u3}^{-}e^{-i\gamma_3\theta})e^{-i\omega t}. \quad (13b)$$

Case IV (*four γ's are real and two γ's are imaginary*):

$$w(\theta,t) = (C_{w1}^{+}e^{-i\gamma_1\theta} + C_{w2}^{+}e^{i\gamma_2\theta} + C_{w3}^{+}e^{-i\gamma_3\theta} + C_{w1}^{-}e^{i\gamma_1\theta} + C_{w2}^{-}e^{-i\gamma_2\theta} + C_{w3}^{-}e^{i\gamma_3\theta})e^{-i\omega t}, \quad (14a)$$

$$u(\theta,t) = (C_{u1}^{+}e^{-i\gamma_1\theta} + C_{u2}^{+}e^{i\gamma_2\theta} + C_{u3}^{+}e^{-i\gamma_3\theta} + C_{u1}^{-}e^{i\gamma_1\theta} + C_{u2}^{-}e^{-i\gamma_2\theta} + C_{u3}^{-}e^{i\gamma_3\theta})e^{-i\omega t}, \quad (14b)$$

where the coefficients C^{+} and C^{-} denote positive-travelling and negative-travelling waves along the curved beam respectively. Note that the wave solutions for Cases I and II are identical in form, so that they can be treated as a single case for computational purposes.

In the present formulation, $e^{-i\gamma_3\theta}$ and $e^{i\gamma_3\theta}$ represent the wave components in which the extensional mode dominates, as indicated in Fig. 2. It can then be seen that these wave components play an important role in determining the overall wave motion, particularly when $\omega > \omega_c$ (γ_3 is real). However, when $\omega < \omega_c$, these wave components oscillate but spatially decay (γ_3 is complex) or attenuate (γ_3 is imaginary). The contribution of these attenuating wave components to the overall wave motion is small and can be neglected when the distance between the origin of disturbance and the boundary/discontinuity is very large since they decay exponentially with the spatial co-ordinate. Note that when these wave components are attenuating or are neglected over the entire frequency range, the problem becomes essentially the same as the inextensional curved beam model in which the wave motion of Case IV does not exist. In other words, when the curved beam is modelled as inextensional, only one pair of wave components (which are flexural mode dominating waves) propagates and the other two pairs of wave components attenuate when $\omega > 4.1996$ (see Fig. 2(b)). However, for the extensional curved beam model, both the extensional and flexural mode dominant waves propagate when $\omega > \omega_c$. Therefore, the accuracy of the inextensional model for predicting natural or forced vibration frequencies depends strongly on the location of the frequency of interest relative to the cut-off frequency $\omega_c = 1/k$. That is, for example, the accuracy of the nth natural frequency ω_n predicted by the inextensional curved beam model may significantly decrease if ω_n is much higher than ω_c. This is true even for lower vibration modes since the wave components associated with extensional modes dominating are considered as attenuating instead of propagating in the inextensional model.

4. Wave reflection and transmission matrices

When a wave is incident upon a discontinuity such as an intermediate support, a different waveguide, or a boundary, it is reflected and/or transmitted at different rates depending on the properties of the discontinuity. A wave either propagates or attenuates; attenuating waves are called near fields. When the distance between discontinuities is relatively small, near fields play an important role in the wave motions by contributing significant amounts of energy to the total power flow [32]. In this section, reflection and transmission matrices of waves incident upon

various kinds of point discontinuities are derived. These matrices are needed for the wave-train closure principle, which provides a systematic approach to free vibration analysis.

4.1. Wave reflection and transmission at a kinetic discontinuity

Consider a curved beam model constrained at a local co-ordinate $\xi = 0$ as shown in Fig. 3, where M and J_M denote the attached mass and its mass moment of inertia, respectively; K_r denotes the rotational elastic constraint, K_w the transverse, and K_u the tangential. The tangential constraint is applicable since the curved beam is extensional. Based on Eqs. (11)–(14), the wave components are grouped into 3×1 vectors of positive-travelling waves $\mathbf{C}^+$ and negative-travelling waves $\mathbf{C}^-$; i.e.,

$$\mathbf{C}^+ = \begin{Bmatrix} C_1^+ \\ C_2^+ \\ C_3^+ \end{Bmatrix}, \tag{15a}$$

$$\mathbf{C}^- = \begin{Bmatrix} C_1^- \\ C_2^- \\ C_3^- \end{Bmatrix}. \tag{15b}$$

Recall that, depending on k, the extensional curved beam model has four different wave solutions as given by Eqs. (11)–(14). When a set of positive-travelling wave $\mathbf{C}^+$ is incident upon a discontinuity, it gives rise to a set of reflected waves $\mathbf{C}^-$ and transmitted waves $\mathbf{D}^+$. These waves are related by

$$\mathbf{C}^- = \mathbf{r}\mathbf{C}^+, \tag{16a}$$

$$\mathbf{D}^+ = \begin{Bmatrix} D_1^+ \\ D_2^+ \\ D_3^+ \end{Bmatrix} = \mathbf{t}\mathbf{C}^+, \tag{16b}$$

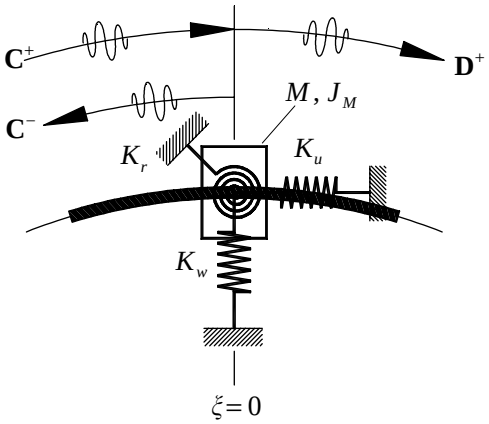

Fig. 3. Wave reflection and transmission at a kinetic discontinuity.

where **r** and **t** are the 3×3 reflection and transmission matrices respectively. By suppressing the temporal terms in the wave solutions (11)–(14), the transverse displacements w^- and w^+, the tangential displacements u^- and u^+, and the rotational motion of a cross-section ψ^- and ψ^+ at the left and right of the discontinuity ($\xi = 0$), respectively, can be expressed in terms of wave amplitudes of the transverse displacement. For example, in Case II, the resulting equations are

$$w^-(\xi) = C_{w1}^+ e^{-i\gamma_1\xi} + C_{w2}^+ e^{-i\gamma_2\xi} + C_{w3}^+ e^{-i\gamma_3\xi} + C_{w1}^- e^{i\gamma_1\xi} + C_{w2}^- e^{i\gamma_2\xi} + C_{w3}^- e^{i\gamma_3\xi}, \tag{17a}$$

$$u^-(\xi) = \alpha_1 C_{w1}^+ e^{-i\gamma_1\xi} + \alpha_2 C_{w2}^+ e^{-i\gamma_2\xi} + \alpha_3 C_{w3}^+ e^{-i\gamma_3\xi} + \alpha_1 C_{w1}^- e^{i\gamma_1\xi} + \alpha_2 C_{w2}^- e^{i\gamma_2\xi} + \alpha_3 C_{w3}^- e^{i\gamma_3\xi}, \tag{17b}$$

$$\psi^-(\xi) = \frac{dw^-}{d\theta} - u^-, \tag{17c}$$

$$w^+(\xi) = C_{w1}^+ e^{-i\gamma_1\xi} + C_{w2}^+ e^{-i\gamma_2\xi} + C_{w3}^+ e^{-i\gamma_3\xi}, \tag{17d}$$

$$u^+(\xi) = \alpha_1 C_{w1}^+ e^{-i\gamma_1\xi} + \alpha_2 C_{w2}^+ e^{-i\gamma_2\xi} + \alpha_3 C_{w3}^+ e^{-i\gamma_3\xi}, \tag{17e}$$

$$\psi^+(\xi) = \frac{dw^+}{d\theta} - u^+, \tag{17f}$$

where

$$\alpha_n = \frac{i\gamma_n(1+\gamma_n^2 k^2)}{\gamma_n^2(1+k^2) - k^2\omega^2}, \quad n = 1, 2, 3. \tag{17g}$$

Moreover, the normal force $\bar{N}^\pm$, the shear force $\bar{Q}^\pm$, and the bending moment $\bar{M}^\pm$ at the left and right of the discontinuity ($\xi = 0$) can be expressed in terms of wave amplitudes of the transverse displacement by applying the relations

$$\bar{N}^\pm = \frac{\partial u^\pm}{\partial \xi} + w^\pm, \tag{18a}$$

$$\bar{Q}^\pm = \frac{\partial^2 u^\pm}{\partial \xi^2} - \frac{\partial^3 w^\pm}{\partial \xi^3}, \tag{18b}$$

$$\bar{M}^\pm = \frac{\partial u^\pm}{\partial \xi} - \frac{\partial^2 w^\pm}{d\xi^2}. \tag{18c}$$

Introducing the non-dimensional parameters

$$k_u = \frac{K_u R^3}{EI}, \qquad k_w = \frac{K_w R^3}{EI}, \qquad k_r = \frac{K_r R}{EI}, \qquad m = \frac{M}{\rho A R}, \qquad j_m = \frac{J_M}{\rho A R^2}, \tag{19}$$

and by imposing the geometric continuity

$$w^-(0) = w^+(0), \tag{20a}$$

$$u^-(0) = u^+(0), \tag{20b}$$

$$\psi^-(0) = \psi^+(0), \tag{20c}$$

and the force and moment balance conditions at $\xi = 0$,

$$\bar{N}^+ - \bar{N}^- = k^2(k_u u^+ + m\ddot{u}^+), \tag{21a}$$

$$\bar{Q}^+ - \bar{Q}^- = k_w w^+ + m\ddot{w}^+, \tag{21b}$$

$$\bar{M}^- - \bar{M}^+ = k_r \psi^+ + j_m \ddot{\psi}^+, \tag{21c}$$

the following set of matrix equations can be established:

$$\begin{bmatrix} 1 & 1 & 1 \\ -\alpha_1 & -\alpha_2 & -\alpha_3 \\ \alpha_1 - i\gamma_1 & \alpha_2 - i\gamma_2 & \alpha_3 - i\gamma_3 \end{bmatrix} \mathbf{C}^+ + \begin{bmatrix} 1 & 1 & 1 \\ \alpha_1 & \alpha_2 & \alpha_3 \\ -\alpha_1 + i\gamma_1 & -\alpha_2 + i\gamma_2 & -\alpha_3 + i\gamma_3 \end{bmatrix} \mathbf{r}\mathbf{C}^+ = \begin{bmatrix} 1 & 1 & 1 \\ -\alpha_1 & -\alpha_2 & -\alpha_3 \\ \alpha_1 - i\gamma_1 & \alpha_2 - i\gamma_2 & \alpha_3 - i\gamma_3 \end{bmatrix} \mathbf{t}\mathbf{C}^+, \tag{22a}$$

$$\begin{bmatrix} -1 - i\alpha_1\gamma_1 & -1 - \alpha_2\gamma_2 & -1 - \alpha_3\gamma_3 \\ -(\alpha_1 - i\gamma_1)\gamma_1^2 & -(\alpha_2 - i\gamma_2)\gamma_2^2 & -(\alpha_3 - i\gamma_3)\gamma_3^2 \\ (\gamma_1 + i\alpha_1)\gamma_1 & (\gamma_2 + i\alpha_2)\gamma_2 & (\gamma_3 + i\alpha_3)\gamma_3 \end{bmatrix} \mathbf{C}^+ + \begin{bmatrix} -1 - i\alpha_1\gamma_1 & -1 - \alpha_2\gamma_2 & -1 - \alpha_3\gamma_3 \\ (\alpha_1 - i\gamma_1)\gamma_1^2 & (\alpha_2 - i\gamma_2)\gamma_2^2 & (\alpha_3 - i\gamma_3)\gamma_3^2 \\ (\gamma_1 + i\alpha_1)\gamma_1 & (\gamma_2 + i\alpha_2)\gamma_2 & (\gamma_3 + i\alpha_3)\gamma_3 \end{bmatrix} \mathbf{r}\mathbf{C}^+ = \begin{bmatrix} -1 - (k^2 c_u + i\gamma_1)\alpha_1 & -1 - (k^2 c_u + i\gamma_2)\alpha_2 & -1 - (k^2 c_u + i\gamma_3)\alpha_3 \\ c_w - (\alpha_1 - i\gamma_1)\gamma_1^2 & c_w - (\alpha_2 - i\gamma_2)\gamma_2^2 & c_w - (\alpha_3 - i\gamma_3)\gamma_3^2 \\ (\alpha_1 - i\gamma_1)(c_r + i\gamma_1) & (\alpha_2 - i\gamma_2)(c_r + i\gamma_2) & (\alpha_3 - i\gamma_3)(c_r + i\gamma_3) \end{bmatrix} \mathbf{t}\mathbf{C}^+, \tag{22b}$$

where

$$c_u = k^2(k_u - m\omega^2), \tag{22c}$$

$$c_w = k_w - m\omega^2, \tag{22d}$$

$$c_r = k_r - j_m\omega^2. \tag{22e}$$

By solving Eq. (22), the reflection and transmission matrices, **r** and **t**, are obtained. Note that since there are four different wave motions in the extensional curved beam model, a different set of **r** and **t** must be derived for each case, using the same procedure described above.

4.2. Wave reflection and transmission at a curvature change

Consider the curved beam model with two elements of different curvatures joined at $\xi = 0$ as shown in Fig. 4. For simplicity, assume that the cross-sectional areas and material properties ρ and E of the two beam elements are the same. Note that the procedure described here is the same even if the areas and/or material properties are different. Let the subscripts l and r denote

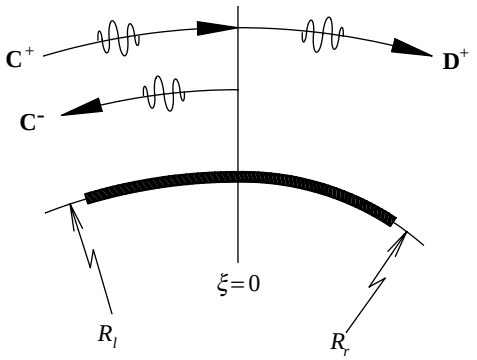

Fig. 4. Wave reflection and transmission at a curvature change.

$\xi = 0^-$ and $\xi = 0^+$ regions, respectively, and $\sigma = R_r/R_l$ (curvature ratio). Then, the modified dispersion equation on the right side of the discontinuity is

$$\gamma_r^6 + (-2 - \sigma^2 k^2 \omega^2)\gamma_r^4 + \{1 - (\sigma^2 + k^2)\sigma^2\omega^2\}\gamma_r^2 + (\sigma^2 k^2 \omega^2 - 1)\sigma^4\omega^2 = 0. \tag{23}$$

A detailed derivation of this equation can be found in Appendix A. It is possible that a wave propagating in $\xi = 0^-$ becomes attenuating after crossing the discontinuity and vice versa since the wave motion on both sides of the discontinuity, in general, can be different depending on the frequency and curvature parameter k. Therefore, for an extensional curved beam, there are mathematically 16 possible combinations of wave motions to be considered since each side of the discontinuity has four wave motions, Cases I–IV. However, since Cases I and II have identical forms for their wave solutions, the actual number of combinations to be considered is nine.

To illustrate the formulation of the wave reflection and transmission matrices, suppose that waves are travelling from the left to right and the wave motion in $\xi = 0^-$ and $\xi = 0^+$ are of Cases II (or I) and III respectively. Then imposing the geometric continuity and force and moment balance at the discontinuity leads to the following matrix equations:

$$\begin{aligned}
&\begin{bmatrix} 1 & 1 & 1 \\ -\alpha_{1l} & -\alpha_{2l} & -\alpha_{3l} \\ \alpha_{1l} - \mathrm{i}\gamma_{1l} & \alpha_{2l} - \mathrm{i}\gamma_{2l} & \alpha_{3l} - \mathrm{i}\gamma_{3l} \end{bmatrix} \mathbf{C}^+ \\
&\quad + \begin{bmatrix} 1 & 1 & 1 \\ \alpha_{1l} & \alpha_{2l} & \alpha_{3l} \\ -\alpha_{1l} + \mathrm{i}\gamma_{1l} & -\alpha_{2l} + \mathrm{i}\gamma_{2l} & -\alpha_{3l} + \mathrm{i}\gamma_{3l} \end{bmatrix} \mathbf{r}_{\mathrm{II-III}} \mathbf{C}^+ \\
&\quad = \begin{bmatrix} 1 & 1 & 1 \\ -\alpha_{1r} & \alpha_{2r} & \alpha_{3r} \\ \sigma^{-1}(\alpha_{1r} - \mathrm{i}\gamma_{1r}) & -\sigma^{-1}(\alpha_{2r} - \mathrm{i}\gamma_{2r}) & -\sigma^{-1}(\alpha_{3r} - \mathrm{i}\gamma_{3r}) \end{bmatrix} \mathbf{t}_{\mathrm{II-III}} \mathbf{C}^+, \qquad (24a)
\end{aligned}$$

$$\begin{bmatrix} -1-\mathrm{i}\alpha_{1l}\gamma_{1l} & -1-\alpha_{2l}\gamma_{2l} & -1-\alpha_{3l}\gamma_{3l} \\ -(\alpha_{1l}-\mathrm{i}\gamma_{1l})\gamma_{1l}^2 & -(\alpha_{2l}-\mathrm{i}\gamma_{2l})\gamma_{2l}^2 & -(\alpha_{3l}-\mathrm{i}\gamma_{3l})\gamma_{3l}^2 \\ (\gamma_{1l}+\mathrm{i}\alpha_{1l})\gamma_{1l} & (\gamma_{2l}+\mathrm{i}\alpha_{2l})\gamma_{2l} & (\gamma_{3l}+\mathrm{i}\alpha_{3l})\gamma_{3l} \end{bmatrix} \mathbf{C}^+$$
$$+ \begin{bmatrix} -1-\mathrm{i}\alpha_{1l}\gamma_{1l} & -1-\alpha_{2l}\gamma_{2l} & -1-\alpha_{3l}\gamma_{3l} \\ (\alpha_{1l}-\mathrm{i}\gamma_{1l})\gamma_{1l}^2 & (\alpha_{2l}-\mathrm{i}\gamma_{2l})\gamma_{2l}^2 & (\alpha_{3l}-\mathrm{i}\gamma_{3l})\gamma_{3l}^2 \\ (\gamma_{1l}+\mathrm{i}\alpha_{1l})\gamma_{1l} & (\gamma_{2l}+\mathrm{i}\alpha_{2l})\gamma_{2l} & (\gamma_{3l}+\mathrm{i}\alpha_{3l})\gamma_{3l} \end{bmatrix} \mathbf{r}_{\mathrm{II-III}}\mathbf{C}^+$$
$$= \begin{bmatrix} -\sigma^{-1}(1+\mathrm{i}\alpha_{1r}\gamma_{1r}) & -\sigma^{-1}(1+\mathrm{i}\alpha_{2r}\gamma_{2r}) & -\sigma^{-1}(1+\mathrm{i}\alpha_{3r}\gamma_{3r}) \\ -\sigma^{-3}(\alpha_{1r}-\mathrm{i}\gamma_{1r})\gamma_{1r}^2 & \sigma^{-3}(\alpha_{2r}-\mathrm{i}\gamma_{2r})\gamma_{2r}^2 & \sigma^{-3}(\alpha_{3r}-\mathrm{i}\gamma_{3r})\gamma_{3r}^2 \\ \sigma^{-2}(\gamma_{1r}+\mathrm{i}\alpha_{1r})\gamma_{1r} & \sigma^{-2}(\gamma_{2r}+\mathrm{i}\alpha_{2r})\gamma_{2r} & \sigma^{-2}(\gamma_{3r}+\mathrm{i}\alpha_{3r})\gamma_{3r} \end{bmatrix} \mathbf{t}_{\mathrm{II-III}}\mathbf{C}^+, \tag{24b}$$

where the subscripts II–III of **r** and **t** denote a transition of wave solutions from Cases II to III. Note that the amplitude ratio α_r on the right side of the discontinuity is also modified as

$$\alpha_{nr} = \frac{\mathrm{i}\gamma_{nr}(\sigma^2+\gamma_{nr}^2k^2)}{\gamma_{nr}^2(\sigma^2+k^2)-\sigma^4k^2\omega^2}, \quad n=1,2,3. \tag{25}$$

By solving Eq. (24), $\mathbf{r}_{\mathrm{II-III}}$ and $\mathbf{t}_{\mathrm{II-III}}$ are obtained. The reflection and transmission matrices for other wave solution combinations can be obtained in a similar manner.

4.3. Wave reflection and transmission at a boundary

Consider an arbitrary boundary condition with translational and rotational springs and an attached mass as shown in Fig. 5. By imposing the force and moment balance at the boundary,

$$\bar{N}^- = -k^2(k_u u^+ + m\ddot{u}^+), \tag{26a}$$

$$\bar{Q}^- = -(k_w w^+ + m\ddot{w}^+), \tag{26b}$$

$$\bar{M}^- = k_r\frac{\partial w^+}{\partial\xi} + j_m\frac{\partial\ddot{w}^+}{\partial\xi}, \tag{26c}$$

the reflection matrix can be derived for each case. For example, $\mathbf{r}_{\mathrm{II}}$ for Case II is

$$\mathbf{r}_{\mathrm{II}} = M_1^{-1}M_2, \tag{27}$$

$$\mathbf{M}_1 = \begin{bmatrix} 1+(k^2c_u+\mathrm{i}\gamma_1)\alpha_1 & 1+(k^2c_u+\mathrm{i}\gamma_2)\alpha_2 & 1+(k^2c_u+\mathrm{i}\gamma_3)\alpha_3 \\ c_w-(\alpha_1+\mathrm{i}\gamma_1)\gamma_1^2 & c_w-(\alpha_2+\mathrm{i}\gamma_2)\gamma_2^2 & c_w-(\alpha_3+\mathrm{i}\gamma_3)\gamma_3^2 \\ (\gamma_1+\mathrm{i}\alpha_1)(-\gamma_1+\mathrm{i}c_r) & (\gamma_2+\mathrm{i}\alpha_2)(-\gamma_2+\mathrm{i}c_r) & (\gamma_3+\mathrm{i}\alpha_3)(-\gamma_{31}+\mathrm{i}c_r) \end{bmatrix}, \tag{28a}$$

$$\mathbf{M}_2 = \begin{bmatrix} -1+(k^2c_u-\mathrm{i}\gamma_1)\alpha_1 & -1+(k^2c_u-\mathrm{i}\gamma_2)\alpha_2 & -1+(k^2c_u-\mathrm{i}\gamma_3)\alpha_3 \\ -c_w-(\alpha_1-\mathrm{i}\gamma_1)\gamma_1^2 & -c_w-(\alpha_2-\mathrm{i}\gamma_2)\gamma_2^2 & -c_w-(\alpha_3-\mathrm{i}\gamma_3)\gamma_3^2 \\ (\gamma_1+\mathrm{i}\alpha_1)(\gamma_1+\mathrm{i}c_r) & (\gamma_2+\mathrm{i}\alpha_2)(\gamma_2+\mathrm{i}c_r) & (\gamma_3+\mathrm{i}\alpha_3)(\gamma_{31}+\mathrm{i}c_r) \end{bmatrix}, \tag{28b}$$

where c_u, c_w, and c_r are given by Eqs. (22c), (22d), and (22e) respectively.

In the limiting cases where the elastic constraints and inertia approach infinity and/or zero, the reflection matrices for the typical classical boundary conditions such as hinged ($k_u = k_w = \infty$ and

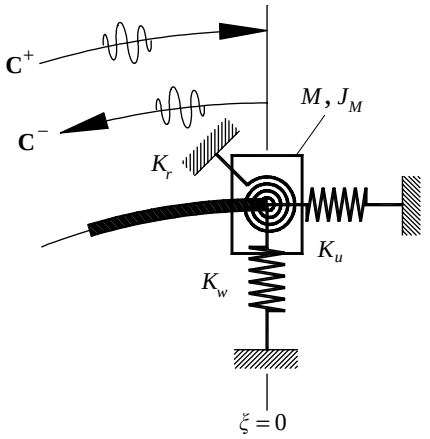

Fig. 5. Wave reflection at a general boundary.

$k_r = m = j_m = 0$), clamped ($k_u = k_w = k_r = \infty$ and $m = j_m = 0$), and free ($k_u = k_w = k_r = m = j_m = 0$) are readily obtained. Note that a similar technique can also be applied to a rigid intermediate support discussed in Section 4.1.

5. Application: free vibration analysis

The reflection and transmission matrices of waves incident upon point discontinuities are now combined with the transfer matrix method to analyze the free vibration of the curved beam with multiple discontinuities. The technique is known as the phase or wave-train closure principle, and it has been applied to Euler–Bernoulli beams in Refs. [30,32] and axially strained spinning Timoshenko beams in Ref. [22]. In this section, the wave-train closure principle is used to provide a systematic approach to the free vibration analysis of curved beams. However, due to the complexity of wave motions in the extensional curved beam model, care must be taken in applying the proper reflection and transmission matrices so that they are consistent with the wavenumbers on both sides of the discontinuity.

Consider a curved beam with constant R with n discontinuities and arbitrary boundaries as shown in Fig. 6. Define $\mathbf{R}_i$ as a generalized reflection matrix which relates the amplitudes of negative and positive travelling waves at station (discontinuity) i and $\mathbf{T}_i$ as the field transfer matrix between station i and $i+1$ which relates the wave amplitudes by

$$\mathbf{w}^+(\theta_0 + \theta) = \mathbf{T}\mathbf{w}^+(\theta_0) \quad \text{or} \quad \mathbf{w}^-(\theta_0 + \theta) = \mathbf{T}^{-1}\mathbf{w}^-(\theta_0), \tag{29}$$

where

$$\mathbf{T} = \begin{bmatrix} e^{-i\gamma_1\theta} & 0 & 0 \\ 0 & e^{-i\gamma_2\theta} & 0 \\ 0 & 0 & e^{-i\gamma_3\theta} \end{bmatrix} \quad \text{for Cases I and II,} \tag{30}$$

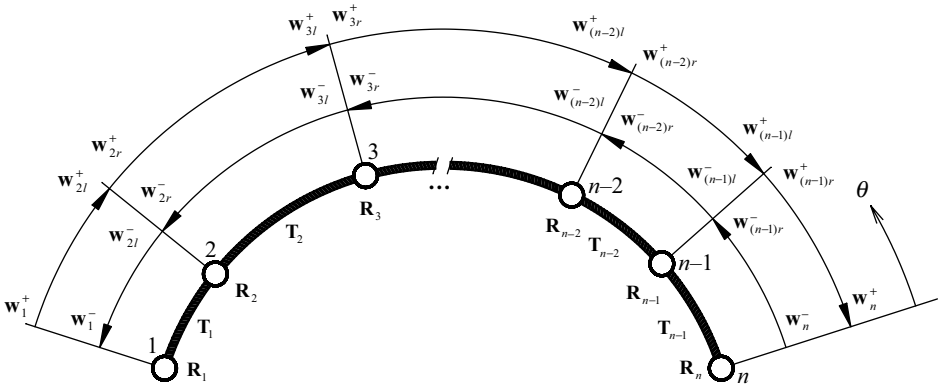

Fig. 6. Curved beam with multiple discontinuities and arbitrary boundary conditions.

$$\mathbf{T} = \begin{bmatrix} e^{-i\gamma_1\theta} & 0 & 0 \\ 0 & e^{i\gamma_2\theta} & 0 \\ 0 & 0 & e^{i\gamma_3\theta} \end{bmatrix} \quad \text{for Case III,} \tag{31}$$

$$\mathbf{T} = \begin{bmatrix} e^{-i\gamma_1\theta} & 0 & 0 \\ 0 & e^{i\gamma_2\theta} & 0 \\ 0 & 0 & e^{-i\gamma_3\theta} \end{bmatrix} \quad \text{for Case IV.} \tag{32}$$

Based on these definitions, the following relations can be found:

$$\mathbf{w}_n^- = \mathbf{R}_n \mathbf{w}_n^+ \quad (\mathbf{R}_n = \mathbf{r}_n), \tag{33}$$

$$\mathbf{w}_{ij}^- = \mathbf{R}_{ij}\mathbf{w}_{ij}^+, \quad \begin{cases} i = 2, 3, \ldots, n-1 \text{ (station number)}, \\ j = l \text{ (left) or } r \text{ (right)}, \end{cases} \tag{34}$$

$$\mathbf{w}_1^- = \mathbf{T}_1 \mathbf{w}_{2l}^-, \tag{35}$$

$$\mathbf{w}_1^+ = \mathbf{R}_1 \mathbf{w}_1^- \quad (\mathbf{R}_1 = \mathbf{r}_1), \tag{36}$$

$$\mathbf{w}_{2l}^+ = \mathbf{T}_1 \mathbf{w}_1^+, \tag{37}$$

where, in Eq. (34),

$$\mathbf{R}_{il} = \mathbf{r}_i + \mathbf{t}_i(\mathbf{R}_{ir}^{-1} - \mathbf{r}_i)^{-1}\mathbf{t}_i, \tag{38a}$$

$$\mathbf{R}_{ir} = \mathbf{T}_i \mathbf{R}_{(i+1)l} \mathbf{T}_i. \tag{38b}$$

For waves travelling across a curvature change, the formulation of $\mathbf{R}_{il}$ requires particular attention. For example, if the wave motions in spans 1 and 2 in Fig. 6 are governed by Cases II

and III, respectively, then, the incoming and outgoing waves at station 2 are related by

$$\mathbf{w}_{2r}^{+} = \mathbf{t}_{\mathrm{II-III}}\mathbf{w}_{2l}^{+} + \mathbf{r}_{\mathrm{III-II}}\mathbf{w}_{2r}^{-}, \tag{39a}$$

$$\mathbf{w}_{2l}^{-} = \mathbf{t}_{\mathrm{III-II}}\mathbf{w}_{2l}^{-} + r_{\mathrm{II-III}}\mathbf{w}_{2l}^{+}, \tag{39b}$$

Since $\mathbf{w}_{2r}^{-} = \mathbf{R}_{2r}\mathbf{w}_{2r}^{+}$, Eqs. (39a) and (39b) can be combined to give

$$\mathbf{w}_{2l}^{-} = \mathbf{R}_{2l}\mathbf{w}_{2r}^{+}, \quad \text{where } \mathbf{R}_{2l} = \mathbf{r}_{\mathrm{II-III}} + \mathbf{t}_{\mathrm{III-II}}(\mathbf{R}_{2r}^{-1} - \mathbf{r}_{\mathrm{III-II}})^{-1}\mathbf{t}_{\mathrm{II-III}}. \tag{40}$$

Therefore, for a geometric discontinuity that alters the wavenumbers, two sets of wave reflection and transmission matrices are necessary to formulate $\mathbf{R}$. Note that, for geometrically uniform spans, Eq. (40) reduces to Eq. (38a). Solving Eqs. (33)–(37) gives

$$(\mathbf{R}_1\mathbf{T}_1\mathbf{R}_{2l}\mathbf{T}_1 - \mathbf{I}_{3\times3})\mathbf{w}_1^{+} = 0, \tag{41}$$

where $\mathbf{I}_{3\times3}$ is the 3×3 identity matrix. For non-trivial solutions, the natural frequencies are obtained from the characteristic equation

$$C(\omega) = \mathrm{Det}[\mathbf{R}_1\mathbf{T}_1\mathbf{R}_{2l}\mathbf{T}_1 - \mathbf{I}_{3\times3}] = 0. \tag{42}$$

When the curved beam is geometrically uniform and has homogeneous material properties in all spans, a single solution form at a given frequency governs the wave motions. In this case, since the wavenumbers are identical for all the spans, formulation of $C(\omega)$ is straightforward. However, in general, one needs to consider multiple wave solutions in the spans, depending on the frequencies and the properties of the discontinuities. Hence, in the derivation of $C(\omega)$, the wave reflection and transmission matrices at each station and the field transfer matrix for each span must be properly determined.

6. Examples

Four examples are presented to demonstrate the application of the wave-train closure principle. Unless otherwise specified, the curvature parameter for all examples is $k = 0.0289$. The first example, which is presented to illustrate the transition between different wave motions, is a single span curved beam with both ends clamped. A schematic of the system is shown on the top of Fig. 7. The value of the span angle is $\theta_0 = 180^\circ$. Fig. 7 shows the plot of $C(\omega)$. It can be seen that the frequencies at which $\mathrm{Re}[C(\omega)] = 0$ and $\mathrm{Im}[C(\omega)] = 0$ are the natural frequencies of the given system. Note the abrupt change in slope of $C(\omega)$ at $\omega = 4.164$ and $\omega = \omega_c = 34.641$. Below $\omega = 4.164$, the wave motion consists of two propagating and four spatially decaying wave components (Case II), while for $4.164 < \omega < \omega_c$, the wave motion consists of two propagating and four attenuating (near field) wave components (Case III). Similarly, for $\omega > \omega_c = 34.641$, the wave motion consists of four propagating and two attenuating wave components (Case IV).

To assess the wave motion behavior of both the extensional and inextensional models over a broad range of span angles, Table 1 is presented. For the previous example of $\theta_0 = 180^\circ$ with clamped ends, it can be seen that the first four natural frequencies fall into Case III. Furthermore, all the frequencies are below the cut-off frequency and there is no significant difference between the extensional and inextensional frequencies. It can be also observed that as θ_0 increases, the natural frequencies of the lower modes begin to appear in the frequency range of Case II, with

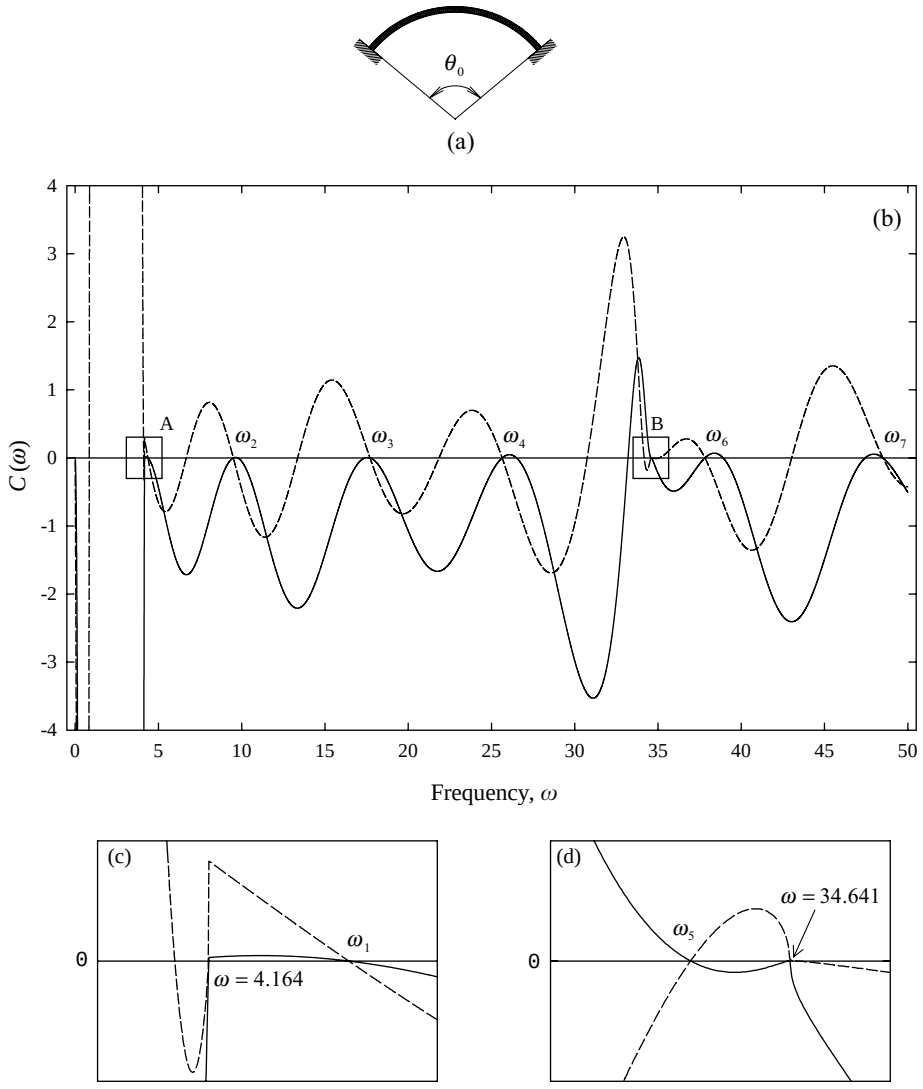

Fig. 7. Results for a one-span extensional curved beam with clamped–clamped ends for $k = 0.0289$ and $\theta_0 = 180^\circ$; Re[$C(\omega)$] (—) and Im[$C(\omega)$] (- - -); (a) schematic of beam model; (b) plot of $C(\omega)$; (c) detail A; (d) detail B.

better agreement existing between the two models. However, as θ_0 decreases, the first natural frequency appears in the frequency range of Case IV in which the extensional waves play an important role in governing the overall wave motion of the curved beam. Considering the case $\theta_0 = 59^\circ$, the first natural frequency predicted by the extensional curved beam model is $\omega_1 = 35.0024$, which is greater than ω_c. However, the inextensional curved beam predicts the first natural frequency to be $\omega_1 = 55.6591$.

The discrepancy between the extensional and inextensional models can be explained by examining the locations of the inextensional natural frequencies relative to the cut-off frequency $\omega_c = 1/k$ of the extensional model. This relative location depends on both the span angle and the

Table 1
Non-dimensional natural frequencies of a curved beam for $k = 0.0289$ ($\omega_c = 34.641$)

Span angle	Mode	Clamped–clamped		Hinged–hinged		Free–free[a]	
(θ_0)		Inextensional	Extensional	Inextensional	Extensional	Inextensional	Extensional
5°	1	8095.7848	1247.5675	5181.5009	1246.8388	8095.7848	1247.1131
	2	14572.946	2489.7481	11067.889	1295.9490	14572.946	2493.9771
	3	26240.991	3740.4334	20733.501	2494.4200	26240.991	2937.7679
	4	38009.405	4987.9286	31835.273	3740.2156	38009.405	3741.4749
45°	1	97.432713	45.682504	61.572909	34.803987	97.432713	35.432205
	2	178.17004	95.832214	134.85983	61.049993	178.17004	98.691915
	3	321.06201	142.99514	253.54899	142.25101	321.06201	143.04121
	4	467.36686	194.12745	391.21460	142.46441	467.36686	194.39288
90°	1	22.625115	22.443037	13.763689	13.687305	22.625115	8.3820157
	2	43.256121	28.112525	32.403584	27.419358	43.256121	23.889413
	3	78.234248	69.653873	61.672635	38.868229	78.234248	47.718346
	4	115.43272	84.655912	96.446257	60.086931	115.43272	77.543681
180°	1	4.3844300	4.3694551	2.2667421	2.2613307	4.3844300	1.8363460
	2	9.6518967	9.4982704	6.9232972	6.8784843	9.6518967	5.3028579
	3	17.921790	17.704014	13.977669	13.889360	17.921790	11.099972
	4	27.523890	25.641709	22.819563	22.334366	27.523890	18.988464
360°	1	0.5664213	0.5661784	0.0000000	0.0000000	0.5664213	0.4376149
	2	1.5952033	1.5925419	0.9007386	0.8997446	1.5952033	0.9517570
	3	3.3845855	3.3749576	2.4466031	2.4417907	3.3845855	2.1366521
	4	5.7649247	5.7302369	4.5966736	4.5843184	5.7649247	3.9645575

[a] Rigid body modes are excluded. Note that there are three rigid body modes in an extensional curved beam with free–free boundary conditions.

curvature parameter k. In general, there will be significant error associated with the inextensional natural frequencies if they are above the cut-off frequency. However, depending upon boundary conditions, if the inextensional natural frequencies are *sufficiently* lower than the cut-off frequency, the inextensional and extensional natural frequencies are comparable. For example, in Table 1, it is observed that the free–free boundary conditions show a relatively large discrepancy between the extensional and inextensional models regardless of whether the natural frequencies are above or below the cut-off frequency. It is also noted that the non-zero natural frequencies of the inextensional curved beam with free–free boundary condition are identical to those of the clamped–clamped case. However, for the extensional curved beam model, they are significantly different due to the effects of the extensional mode, which provides an additional degree of freedom to the beam. An analogous behavior can be observed in straight beams where the clamped–clamped and free–free boundary conditions for an Euler–Bernoulli beam are identical, while for the Timoshenko beam they are different.

The second example is a two-span extensional curved beam with an intermediate elastic support as depicted in Fig. 8. The intermediate support consists of three point springs which constraint the transverse motion in the w direction, the translational motion in the u direction, and the rotational motion of the cross-sectional element. The total angle of the curved beam is 180° and the angles of the two sub-spans are $\theta_1 = 111.6°$ and $\theta_2 = 68.4°$. Both ends of the beam are hinged. As seen in

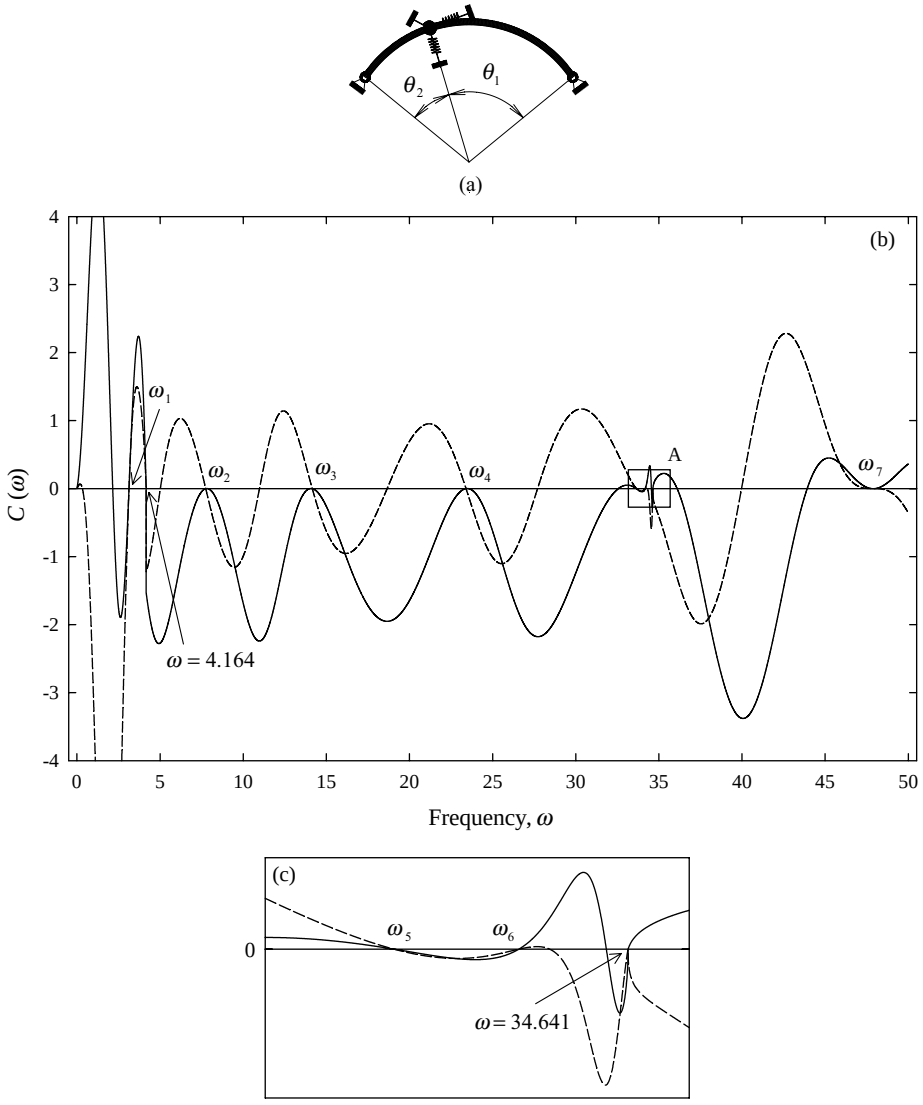

Fig. 8. Results for a two-span extensional curved beam with elastic support and hinged ends for $k = 0.0289$, $k_u = 10$, $k_w = 10$, $k_r = 5$, $\theta_1 = 111.6^\circ$ and $\theta_2 = 68.4^\circ$; Re[$C(\omega)$] (—) and Im[$C(\omega)$] (- - -); (a) schematic of beam model; (b) plot of $C(\omega)$; (c) detail A.

Table 2, the natural frequencies predicted by the inextensional curved beam are higher than those from the extensional curved beam and the difference between the two models increases significantly when frequencies are above the cut-off frequency ω_c. However, it should be noted that the effects of rotary inertia and shear deformation on natural frequencies are more pronounced in higher vibration modes and these effects, which are not included in the present analysis, may be required in the formulation for more accurate results. Also note that the modular nature of the wave reflection and transmission matrices presented in this paper allow various

Table 2
Non-dimensional natural frequencies of the two-span curved beam in Fig. 8

Mode	Inextensional	Extensional
1	3.1355520	3.1302945
2	7.7944178	7.7405333
3	14.235502	14.1521194
4	23.926261	23.4005797
5	34.528830	33.6470200
6	47.146488	34.1769670
7	63.196015	47.8112102

combinations of intermediate supports and boundary conditions to be applied, as illustrated in the following example.

The third example shows the plot of $C(\omega)$ for the extensional curved beam with an intermediate elastic support and a point mass. The beam is also supported by springs at both ends. A schematic of the system is depicted in Fig. 9(a). The total angle of the beam is 180° and the span angles of the three sub-spans are $\theta_1 = 57.6^\circ$, $\theta_2 = 45^\circ$, and $\theta_3 = 77.4^\circ$. Note that in general the point mass decreases the transmission and increases the reflection of the waves, and that at very high frequencies, there is essentially no wave transmission [33]. In Figs. 9 and 10, it is seen that small frequency increments $\Delta\omega$ may be required to find the roots of $C(\omega)$ due to the drastic variations in $C(\omega)$ which are caused by some of the eigenvalues of the individual sub-spans being close to the eigenvalues of the entire beam system or because the subsystems are weakly coupled through the intermediate support. Although the plot of $C(\omega)$ indicates sharp jumps near the natural frequencies, the functions remain continuous and finite as shown in Fig. 10 so that there are no difficulties in finding the roots.

The fourth example is an extensional curved beam with three sub-spans of equal span angle but different radius of curvature. A schematic of the system is depicted in Fig. 11(a). The total span angle is 180° and each sub-span angle is 60° for the given geometry. In this example, the form of the wave solution changes from one sub-span to another and as the frequency is varied. Fig. 12 outlines a general flow chart for computing $C(\omega)$. In the flow chart, $\omega_{c1}^{(n)}$ and $\omega_{c2}^{(n)}$ are the critical frequencies at which the wave motion changes from Case II to III and from Case III to IV, respectively, in the nth sub-span. The cut-off frequencies $\omega_{c1}^{(n)}$ can be readily obtained from the dispersion equation by solving for the frequency at which four complex wavenumbers change to imaginary ones, and $\omega_{c2}^{(n)} = k_n^{-1}$. The problem presented here has also been solved by applying the finite element method (FEM) [19,34] and the cells discretization method (CDM) [34]. In Table 3, the non-dimensional natural frequencies obtained from the present approach are compared with those of references [19,34]. Note that the natural frequencies obtained from the present wave analysis are exact since both propagating and attenuating wave components are considered in the formulation.

It should be noted that the present wave approach always results in evaluating the determinant of a 3×3 matrix (see Eq. (42)) regardless of the number of sub-spans. However, a matrix of size $6n \times 6n$ (n is the number of sub-spans) needs to be considered if one applies the classical method of separation of variables, which may cause strenuous computations associated with large-order

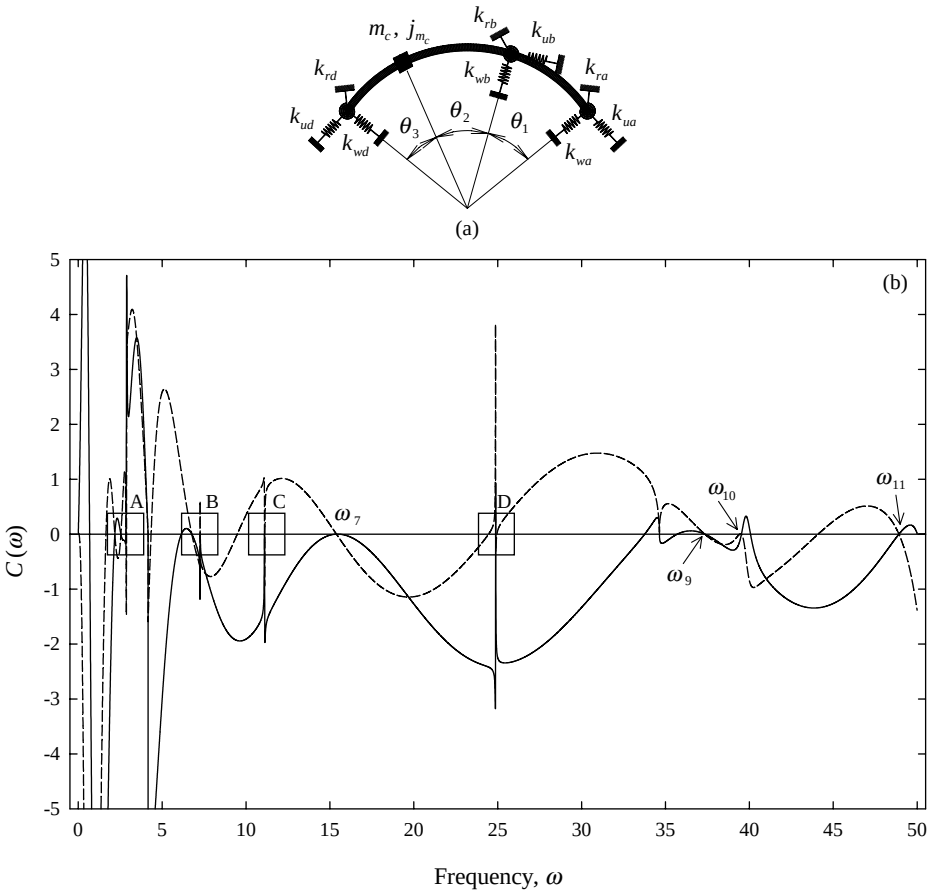

Fig. 9. Results for a three-span extensional curved beam with elastic supports and boundaries for $k = 0.0289$, $\theta_1 = 57.6^\circ$, $\theta_2 = 45^\circ$, $\theta_3 = 77.4^\circ$, $k_{ua} = 30$, $k_{wa} = 30$, $k_{ra} = 20$, $k_{ub} = k_{ud} = 20$, $k_{wb} = k_{wd} = 20$, $k_{rb} = k_{rd} = 10$, $m_c = 3$, and $j_{m_c} = 1$; Re[$C(\omega)$] (—) and Im[$C(\omega)$] (- - -); (a) schematic of beam model; (b) plot of $C(\omega)$. See Fig. 10 for the enlarged views at A, B, C, and D.

matrices. In Fig. 13, the wave approach is compared to the classical method of separation of variables by plotting $C(\omega)$ for the two-span inextensional curved beam. It is seen that the classical method of separation of variable results in very large values of $C(\omega)$ as well as very large slopes near the natural frequencies. For this example, the maximum order of the amplitude of $C(\omega)$ by the method of separation of variables is 10^{28} within the given range of frequencies. This makes the search for the roots of $C(\omega)$ extremely difficult since the convergence of most root-finding routines (e.g., Newton–Raphson method or secant method) depends strongly on the slope of the curve near the roots. Although both approaches lead to the same roots, the wave approach produces a different characteristic equation from which the natural frequencies can be more easily obtained. Mead [30] also showed that the phase closure principle led to a different characteristic equation for the Euler–Bernoulli beam. As pointed by Mace [32], the only source of numerical difficulty in this wave approach occurs when flexural components of the whole system contain an insignificant

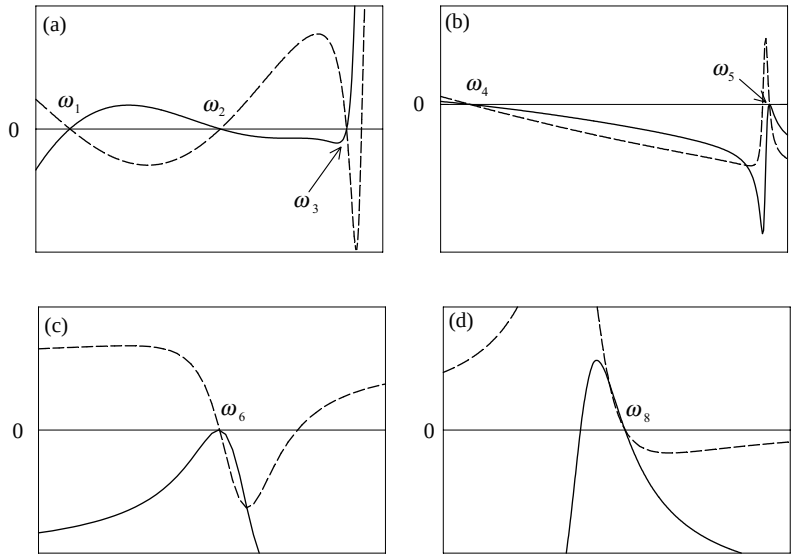

Fig. 10. Enlarged views of $C(\omega)$ at the indicated locations in Fig. 9; (a) detail A; (b) detail B; (c) detail C; (d) detail D.

Table 3
Non-dimensional natural frequencies of the three-span curved beam in Fig. 11

Mode	Present	FEM			CDM
		12 curved elements		24 straight elements	100 degrees of freedom
		Ref. [34]	Ref. [19]	Ref. [34]	Ref. [34]
1	2.6833155	2.680	2.701	2.685	2.671
2	4.8337572	4.824	4.828	4.828	4.780
3	9.5647244	9.536	9.543	9.543	9.413
4	14.5850042	14.527	14.535	14.535	14.309
5	21.8646005	21.749	21.751	21.751	21.265

amount of the total mass or flexibility of the system. In this case, the beam spans then appear physically as rigid bodies or massless elements, resulting in the wavenumber becoming very small, and thus the representation of the beam displacement in terms of waves becomes unrealistic. This situation leads to significant rounding errors in the computations. In practice, however, the contribution of beam mass and flexibility are usually large enough to avoid this difficulty.

7. Summary and conclusions

In this paper, a systematic approach based on wave propagation is presented to study the free vibration of an extensional/inextensional multi-span curved beam with general support conditions. For the extensional curved beam, there exist two frequency branches above the cut-

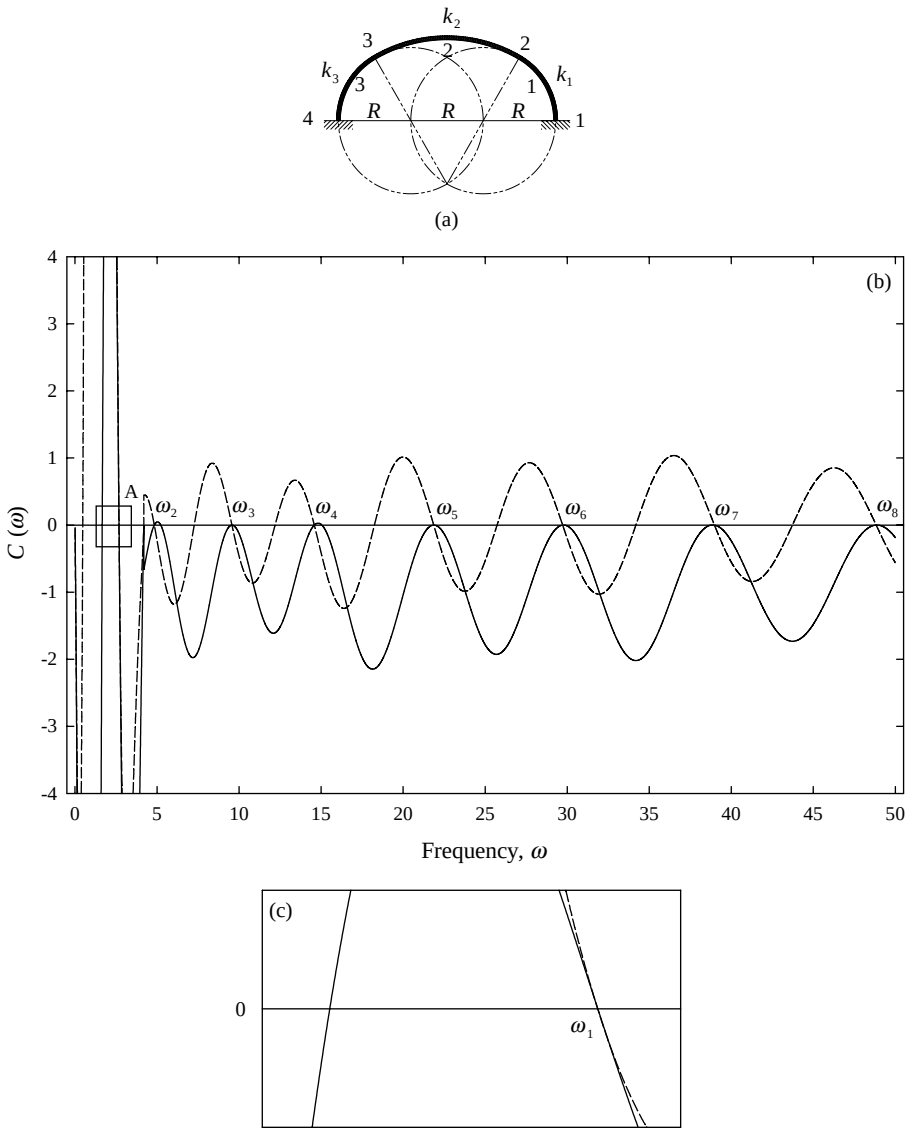

Fig. 11. Results for a three-span extensional curved beam with curvature changes and clamped–clamped ends for $k_1 = k_3 = 0.01$, and $k_2 = 0.02$; Re[$C(\omega)$] (—) and Im[$C(\omega)$] (- - -); (a) schematic of beam model; (b) plot of $C(\omega)$; (c) detail A.

off frequency, with the cut-off frequency being defined as the inverse of the curvature parameter. One branch contains wave components that are flexural mode dominating while the other contains wave components with extensional mode dominating. Based on the nature of the wavenumbers of the six wave components, the wave motions in the extensional curved beam can be classified into four possible types, with each type being represented by a unique harmonic wave

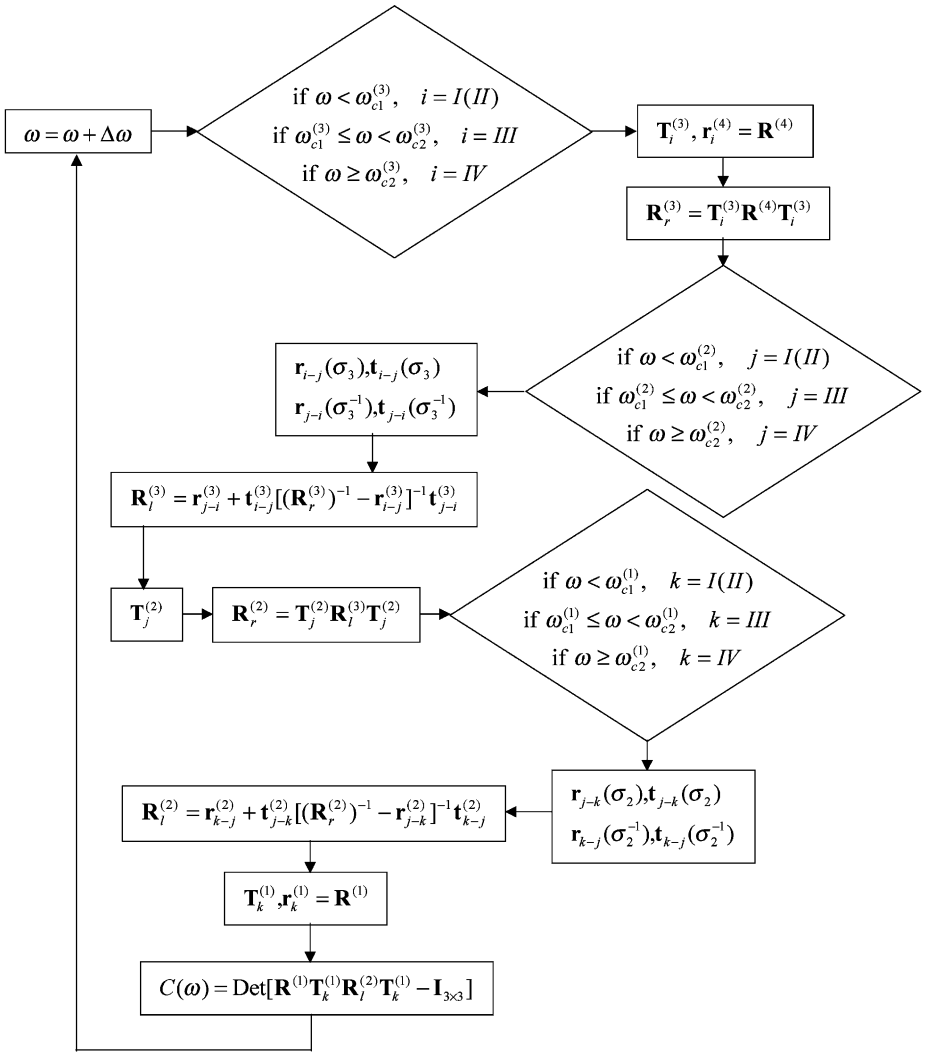

Fig. 12. Algorithm for computing the characteristic equation in example 4. Superscripts denote station numbers (or span numbers for ω_{c1}, ω_{c2}, and $\mathbf{T}$). i, j, and k denote the wave motions of the three cases.

solution. The wave motions at the discontinuities are described by the wave reflection and transmission matrices, which include the effects of attenuating wave components. These wave reflection and transmission matrices are derived for kinetic and geometric discontinuities as well as reflection matrices for various boundary conditions. By applying the wave-train closure principle, the wave reflection and transmission matrices at discontinuities and boundaries are combined with the field transfer matrices, from which characteristic equations of extensional multi-span curved beams are obtained in a systematic manner. The proposed wave approach is exact and results in recursive algorithms that always involve computations of 3×3 matrices

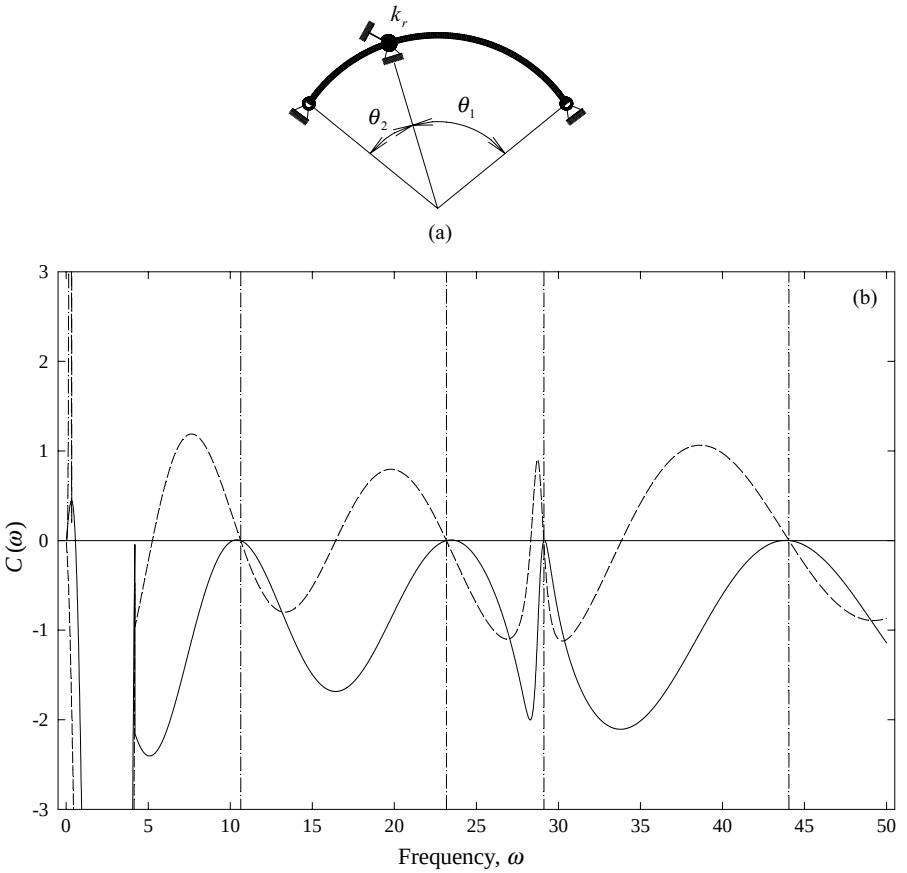

Fig. 13. Comparison of amplitudes and slopes of $C(\omega)$ between the wave approach and standard method of separation of variables for a two-span inextensional curved beam with $\theta_1 = 110^\circ$, $\theta_2 = 70^\circ$, and $k_r = 10$; Re$[C(\omega)]$ (—) and Im$[C(\omega)]$ (- - -). Dot-dashed curve (-··-) shows the result by the standard method of separation of variables; (a) schematic of beam model; (b) plot of $C(\omega)$.

regardless of the number of sub-spans. Four examples are presented to illustrate the procedure and compare the results of the present technique with other methods.

Appendix A. Derivation of the dispersion equation

The equations for the right side ($\xi = 0^+$) of a curved beam with a radius of curvature R, are

$$\frac{EI}{R_r^3}\frac{\partial^3}{\partial\theta^3}\left(U - \frac{\partial W}{\partial\theta}\right) - \frac{EA}{R_r}\left(W + \frac{\partial U}{\partial\theta}\right) = \rho A R_r \frac{\partial^2 W}{\partial T^2}, \tag{A.1a}$$

$$\frac{EI}{R_r^3}\frac{\partial^2}{\partial\theta^2}\left(U - \frac{\partial W}{\partial\theta}\right) + \frac{EA}{R_r}\frac{\partial}{\partial\theta}\left(W + \frac{\partial U}{\partial\theta}\right) = \rho A R_r \frac{\partial^2 U}{\partial T^2}. \tag{A.1b}$$

Upon applying the non-dimensional parameters and variables in Eqs. (2) and (4) with $R = R_l$ and $R_r = \sigma R_l$ to Eq. (A.1), one obtains

$$k^2 \frac{\partial^3}{\partial\theta^3}\left(u - \frac{\partial w}{\partial\theta}\right) - \sigma^2\left(w + \frac{\partial u}{\partial\theta}\right) = -k^2\sigma^4\omega^2 w, \tag{A.2a}$$

$$k^2 \frac{\partial^2}{\partial\theta^2}\left(u - \frac{\partial w}{\partial\theta}\right) + \sigma^2 \frac{\partial}{\partial\theta}\left(w + \frac{\partial u}{\partial\theta}\right) = -k^2\sigma^4\omega^2 u. \tag{A.2b}$$

The harmonic wave solutions of Eq. (A.2) can be assumed as

$$w(\theta, t) = C_w e^{i(\gamma_r\theta - \omega t)}, \tag{A.3a}$$

$$u(\theta, t) = C_u e^{i(\gamma_r\theta - \omega t)}, \quad 0 \leqslant \theta \leqslant 2\pi, \tag{A.3b}$$

where $\gamma_r(k, \omega, \sigma)$ denotes the wavenumber which differs from $\gamma = \gamma_l$. Substitution of the harmonic wave solutions (A.3) into Eq. (A.2) leads to

$$\begin{bmatrix} \sigma^2 + k^2(\gamma_r^4 - \sigma^4\omega^2) & i\gamma_r(\sigma^2 + \gamma_r^2 k^2) \\ i\gamma_r(\sigma^2 + \gamma_r^2 k^2) & -\sigma^2\gamma_r^2 + k^2(\sigma^4\omega^2 - \gamma_r^2) \end{bmatrix} \begin{Bmatrix} C_w \\ C_u \end{Bmatrix} = 0. \tag{A.4}$$

For non-trivial solutions, the dispersion equation is

$$\gamma_r^6 + (-2 - \sigma^2 k^2\omega^2)\gamma_r^4 + \{1 - (\sigma^2 + k^2)\sigma^2\omega^2\}\gamma_r^2 + (\sigma^2 k^2\omega^2 - 1)\sigma^4\omega^2 = 0. \tag{A.5}$$

References

[1] P. Chidamparam, A.W. Leissa, Vibration of planar curved beams, rings, and arches, Applied Mechanics Review 46 (1993) 467–483.

[2] P.A.A. Laura, M.J. Maurizi, Recent research on vibrations of arch-type structures, Shock and Vibration Digest 19 (1987) 6–9.

[3] S. Markus, T. Nanasi, Vibration of curved beams, Shock and Vibration Digest 13 (1981) 3–14.

[4] J.P. Den Hartog, The lowest frequency of circular arcs, Philosophical Magazine 5 (1928) 400–408.

[5] R.E. Ball, Dynamic analysis of rings by finite differences, Journal of the Engineering Mechanics Division American Society of Civil Engineers 93 (1967) 1–10.

[6] S.S. Rao, V. Sundararajan, In-plane flexural vibrations of circular rings, Journal of Applied Mechanics 36 (1969) 620–625.

[7] E. Tufekci, A. Arpaci, Exact solution of in-plane vibrations of circular arches with account taken of axial extension, transverse shear and rotatory inertia effects, Journal of Sound and Vibration 209 (1998) 845–856.

[8] T.M. Wang, J.M. Lee, Natural frequencies of multi-span circular curved frames, International Journal of Solids and Structures 8 (1972) 791–805.

[9] W.B. Bickford, B.T. Strom, Vibration of plane curved beams, Journal of Sound and Vibration 39 (1975) 135–146.

[10] M.S. Issa, T.M. Wang, B.T. Hsiao, Extensional vibrations of continuous circular curved beams with rotary inertia and shear deformation: free vibration, Journal of Sound and Vibration 114 (1987) 297–308.

[11] P. Chidamparam, A.W. Leissa, Influence of centerline extensibility on the in-plane free vibrations of loaded circular arches, Journal of Sound and Vibration 183 (1995) 779–795.

[12] S.T. Mau, A.N. Williams, Green's function solution for arch vibration, Journal of Engineering Mechanics 114 (1988) 1259–1264.

[13] M. Petyt, C.C. Fleischer, Free vibration of a curved beam, Journal of Sound of Vibration 18 (1971) 17–30.

[14] R. Davis, R.D. Henshell, G.B. Warburton, Constant curvature beam finite elements for in-plane vibration, Journal of Sound and Vibration 25 (1972) 561–576.
[15] D.J. Dawe, A finite element for vibration analysis of Timoshenko beams, Journal of Sound and Vibration 60 (1978) 11–20.
[16] G. Prathap, The curved beam/deep arch/finite ring element revisited, International Journal for Numerical Methods in Engineering 21 (1985) 389–407.
[17] G.R. Heppler, An element for studying the vibration of unrestrained curved Timoshenko beams, Journal of Sound and Vibration 158 (1992) 387–404.
[18] S.Y. Yang, H.C. Sin, Curvature-based beam elements for the analysis of Timoshenko and shear-deformable curved beams, Journal of Sound and Vibration 187 (1995) 569–584.
[19] A. Krishnan, Y.J. Suresh, A simple cubic linear element for static and free vibration analyses of curved beams, Computers and Structures 68 (1998) 473–489.
[20] K.F. Graff, Wave Motion in Elastic Solids, Clarendon Press, Oxford, 1975.
[21] L. Cremer, M. Heckl, E.E. Ungar, Structure-borne Sound, Springer, Berlin, 1973.
[22] C.A. Tan, B. Kang, Free vibration of axially loaded, rotating Timoshenko shaft systems by the wave-train closure principle, International Journal of Solids and Structures 36 (1999) 4031–4049.
[23] Y. Yong, Y.K. Lin, Propagation of decaying waves in periodic and piecewise periodic structures of finite length, Journal of Sound and Vibration 129 (1989) 99–118.
[24] A.E.H. Love, A Treatise on the Mathematical Theory of Elasticity, Dover, New York, 1944.
[25] W.H. Wittrick, On elastic wave propagation in helical springs, International Journal of Mechanical Sciences 8 (1966) 25–47.
[26] M. Farshad, Wave propagation in prestressed curved rods, Journal of Engineering Mechanics 106 (1980) 395–408.
[27] L.S.D. Morley, Elastic waves in a naturally curved rod, Quarterly Journal of Mechanics and Applied Mathematics 14 (1961) 155–172.
[28] K.F. Graff, Elastic wave propagation in a curved sonic transmission line, IEEE Transactions on Sonics and Ultrasonics 17 (1970) 1–6.
[29] A.K. Mallik, D.J. Mead, Free vibration of thin circular rings on periodic radial supports, Journal of Sound and Vibration 54 (1977) 13–27.
[30] D.J. Mead, Waves and modes in finite beams: application of the phase-closure principle, Journal of Sound and Vibration 171 (1994) 695–702.
[31] S.J. Walsh, R.G. White, Vibrational power transmission in curved beams, Journal of Sound and Vibration 233 (2000) 455–488.
[32] B.R. Mace, Wave reflection and transmission in beams, Journal of Sound and Vibration 97 (1984) 237–246.
[33] C.A. Tan, B. Kang, Wave reflection and transmission in an axially strained, rotating Timoshenko shaft, Journal of Sound and Vibration 213 (1998) 483–510.
[34] M.J. Maurizi, P.M. Belles, R.E. Rossi, M.A. Rosa, Free vibration of a three-centered arc clamped at the ends, Journal of Sound and Vibration 161 (1993) 187–189.